Taylor & Francis
Taylor & Francis Group

REPORT

Generation and characterization of ABBV642, a dual variable domain immunoglobulin molecule (DVD-Ig) that potently neutralizes VEGF and PDGF-BB and is designed for the treatment of exudative age-related macular degeneration

Kun Ding[a,b,*], Lucia Eaton[c,*], Diana Bowley[d,*], Matthew Rieser[e], Qing Chang[c,d], Maria C. Harris[d], Anca Clabbers[d], Feng Dong[c,d], Jikui Shen[a], Sean F. Hackett[a], Debra S. Touw[d], Jacqueline Bixby[d], Suju Zhong[d], Lorenzo Benatuil[d], Sahana Bose[d], Christine Grinnell[e], Gregory M. Preston[e], Ramesh Iyer[d], Ramkrishna Sadhukhan[d], Susan Marchie [iD][d], Gary Overmeyer[d], Tariq Ghayur[c], Deborah A. van Riet[c], Shibo Tang[f], Peter A. Campochario[a,**], and Jijie Gu[c,d,**]

[a]John Hopkins Wilmer Eye Institute, Baltimore, MD, USA; [b]State Key Laboratory of Ophthalmology, Zhongshan Ophthalmic Center, Sun Yat-sen University, Guangzhou, China; [c]Immunology Discovery, AbbVie Bioresearch Center, Worcester, MA, USA; [d]Global Biologics, AbbVie Bioresearch Center, Worcester, MA, USA; [e]DMPK-BA, AbbVie Inc., Libertyville, IL, USA; [f]Aier School of Ophthalmology, Central South University, Changsha, China

ABSTRACT

Exudative age-related macular degeneration (AMD) is the most common cause of moderate and severe vision loss in developed countries. Intraocular injections of vascular endothelial growth factor (VEGF or VEGF-A)-neutralizing proteins provide substantial benefit, but frequent, long-term injections are needed. In addition, many patients experience initial visual gains that are ultimately lost due to subretinal fibrosis. Preclinical studies and early phase clinical trials suggest that combined suppression of VEGF and platelet-derived growth factor-BB (PDGF-BB) provides better outcomes than suppression of VEGF alone, due to more frequent regression of neovascularization (NV) and suppression of subretinal fibrosis. We generated a dual variable domain immunoglobulin molecule, ABBV642 that specifically and potently binds and neutralizes VEGF and PDGF-BB. ABBV642 has been optimized for treatment of exudative AMD based on the following design characteristics: 1) high affinity binding to all VEGF-A isoforms and both soluble and extracellular matrix (ECM)-associated PDGF-BB; 2) potential for extended residence time in the vitreous cavity to decrease the frequency of intraocular injections; 3) rapid clearance from systemic circulation compared with molecules with wild type Fc region for normal FcRn binding, which may reduce the risk of systemic complications; and 4) low risk of potential effector function. The bispecificity of ABBV642 allows for a single injection of a single therapeutic agent, and thus a more streamlined development and regulatory path compared with combination products. In a mouse model of exudative AMD, ABBV642 was observed to be more effective than aflibercept. ABBV642 has potential to improve efficacy with reduced injection frequency in patients with exudative AMD, thereby reducing the enormous disease burden for patients and society.

Introduction

Age-related macular degeneration (AMD) is a multigenic disease wherein the accumulation of drusen, the atrophy of retinal pigmented epithelial (RPE), and neovascularization can result in the death of photoreceptors and the loss of central vision. This gradual decrease in central vision usually occurs slowly over many years. However, in about 15% of patients, subretinal neovascularization occurs when fluid leaks into or under the macula, which results in rapid and often severe loss of vision. This is called exudative AMD to emphasize the most critical and differentiating feature of this subgroup of patients with AMD, exudation of fluid into the macula.[1] In 2007, the World Health Organization (WHO) estimated that exudative AMD affects 3 million people globally and accounts for 8.7% of all blindness and 50% of blindness in industrialized nations. WHO projects that these numbers will double by 2020 as populations age in many countries.[1]

The conversion from nonexudative to exudative AMD occurs when stabilization of hypoxia-inducible factor-1 (HIF-1) from hypoxia or oxidative stress results in upregulation of VEGF and other vasoactive proteins in macular photoreceptors and RPE cells.[2-5] Intraocular injections of the VEGF neutralizing proteins therapeutics, ranibizumab, aflibercept, or bevacizumab, over the course of two years can substantially improve visual acuity in patients with exudative AMD.[6-9] However, the striking visual acuity gains seen after two years of treatment in a clinical trial were completely lost three years after patients exited the trial and initiated standard care methodologies.[10] Many of the patients who lost initial visual acuity gains had subretinal hyper-reflective material suggestive of subretinal fibrosis or areas of macular atrophy. Subretinal hyper-reflective material is a risk factor for macular atrophy, so one possible hypothesis is that over time many patients develop subretinal fibrosis despite treatment with anti-VEGF agents because other HIF-1-

stimulated vasoactive agent stimulates subretinal fibrosis.[11] PDGF-BB is upregulated by HIF-1, is a chemoattractant for glia and RPE cells and promotes scarring.[12-16] In mouse models of subretinal neovascularization[17,18] and in an early phase clinical trial in patients with exudative AMD, combined suppression of VEGF and PDGF-BB provided superior outcomes versus suppression of VEGF alone, due to more frequent regression of neovascularization and suppression of subretinal fibrosis.[19,20] Thus, there is strong rationale for combined suppression of VEGF and PDGF-BB in patients with exudative AMD.

Here, we report the design, generation and characterization of ABBV642, a dual variable domain immunoglobulin molecule (DVD-Ig) that potently neutralizes both VEGF-A and PDGF-BB and was specifically engineered to improve the safety and convenience of wet AMD treatment. ABBV642 is a drug development candidate; the translation of the design features of ABBV642 into benefits for exudative AMD patients needs to be evaluated in clinical trials.

Results

Design considerations for next-generation treatments for exudative AMD

The efficacy and safety profile of current anti-angiogenesis therapeutics for intraocular use may be improved by engineering more potent or multispecific inhibitors to limit the number of molecules/injections required to achieve the desired therapeutic effect. Three factors were carefully considered in designing a bispecific agent for ocular diseases that targets both VEGF-A and PDGF-BB and provides improved efficacy, as well as improved safety and convenience. The first factor was improved efficacy. Compared to suppression of VEGF alone, combined suppression of VEGF and PDGF-BB caused greater suppression of subretinal NV in mice[17,18] and better outcomes in resolution of choroidal NV and reduced fibrosis in patients with exudative AMD.[19] ABBV642 was design to potently bind and neutralize all VEGF-A isoforms and both soluble and ECM-associated PDGF-BB. Second, we considered the potential for extended residence time in the vitreous cavity. Repeated intravitreal injections increase the risk of endophthalmitis and are a substantial burden for patients, their families, and retina specialists. Increased residence time in the vitreous cavity will increase the duration of efficacy for biologics and decrease the frequency of injections. Increase in molecular size was reported to have a weak correlation with increase in residence time in the vitreous cavity.[21,22,23] A full-length 200 kDa DVD-Ig format with a larger molecular size was therefore selected for ABBV642. The third factor considered was safety. Although prolonged residence time in the eye is desirable, prolonged residence in systemic circulation is not because systemic suppression of VEGF is associated with hemorrhagic and thromboembolic complications.[24] The Fc neonatal receptor (FcRn) is responsible for prolonged serum residence,[25] but is not required for ocular[21,23] half-life of immunoglobulin molecules, and therefore FcRn binding was disabled in ABBV642 by introduction of a H435A (FcRn null) mutation.[26]

Endothelial cells release paracrine PDGF-BB, which is retained proximally by heparin sulfate proteoglycan. This is essential for proper recruitment and organization of pericytes to establish microvessels.[27] VEGF-A is secreted in multiple isoforms with variable affinity for extracellular proteins. Initially, it was thought only the longer isoforms of VEGF189 and VEGF206 are bound in the ECM when they are produced. A somewhat surprising finding was that as much as 50–70% of VEGF165, the most active VEGF-A isoform, could be released by heparin from ECM, suggesting that, although this isoform is secreted, a substantial fraction remains bound to heparin sulfate proteoglycans.[28] Fc effector function is not required for the activity of ABBV642. Hypothetically, the ECM-associated VEGF-A and PDGF-BB may mediate antibody-dependent cell-mediated cytotoxicity (ADCC), complement-dependent cytotoxicity (CDC), or elicit Fc-mediated immune cell cytokine release if they bound to Fc-competent IgG molecules. To provide security against the potential risk of ADCC, CDC, or Fc-mediated immune cell cytokine release, we introduced L234A and L235A mutations at the lower hinge region of ABBV642 to attenuate binding to FcγR I FcγR II and C1q molecules.[29,30] With these design considerations in mind, we generated an anti-VEGF-A/anti-PDGF-BB DVD-Ig molecule with L234A, L235A and H435A mutations, designated as ABBV642 (Fig. 1). As a bispecific, this allows for a single injection and a more streamlined development and regulatory path vs. combination products. We will describe the selection and in vitro and in vivo characterization of ABBV642 below.

Selection of a DVD-Ig molecule with improved thermal stability

We first described the DVD-Ig format in 2007.[31] A DVD-Ig molecule is a dual-specific tetravalent IgG-like molecule with two target binding variable domains on each Fab arm. A DVD-Ig molecule can be generated with variable domains from any two mAbs linked in tandem via naturally occurring linkers or glycine-serine linkers. The tandem linkage of the variable domains and the ability to adjust linker lengths offer tremendous structural and functional flexibility to the DVD-Ig format, such that we can join two variable domains of interest (e.g., different functionalities), adjust the position of the first variable domain and the second variable domains relative to CH1/CL (variable domain orientation), and adjust the distance between the two variable domains (linker design and combinations). Like an optimized therapeutic mAb, an optimized DVD-Ig molecule has many desirable properties, such as acceptable expression in mammalian cells for transient and large-scale production, simple purification to homogeneity using standard approaches, and good drug-like biophysical, biochemical, and pharmacokinetic (PK) properties.[31] Currently, three DVD-Ig molecules, lutikizumab (ABT-981), remtolumab (ABT-122) and ABT-165, are in clinical development.

The CH1/CL domain in a regular IgG molecule not only helps the proper folding of the variable domain, but may also contribute to the stabilization of the variable domain. The major structural difference between a DVD-Ig molecule and a mAb is an additional variable domain on each Fab and linkers connecting the two variable domains in a DVD-Ig molecule. The outer variable domain in some DVD-Ig molecules may not be as stable as in the parental mAb because it is being
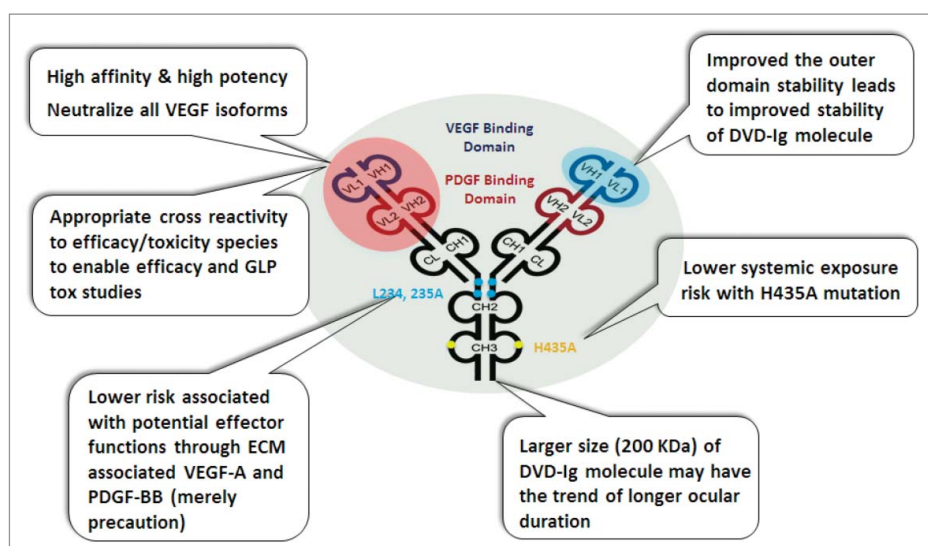
Figure 1. Design features of anti-VEGF-A/anti-PDGF-BB DVD-Ig molecule, ABBV642. VD = variable domain; ECM = extracellular matrix.

supported by VH and VL of the inner variable domain, instead of the CH1/CL. Therefore, if the appropriate CH1/CL stabilization support is not available and the intrinsic stability of VH and VL of the outer variable domain is not strong enough in some DVD-Ig molecules, the outer variable domain may become less stable and may reduce overall stability of the entire molecule. We found that the accelerated storage stability of DVD-Ig molecules is correlated with the Tm value of the highest peak of mAbs used for DVD-Ig outer variable domains (Fig. 2A and B). To this regard, a total of 73 mAbs (45 anti-VEGF-A mAbs and 28 anti-PDGF-BB mAbs) were selected and analyzed by differential scanning calorimetry (DSC) and the thermal stabilities of their VH-VL regions were quantitated by determining the temperature of the highest peak in the DSC thermograms. We selected the mAbs with higher VH and VL thermal stabilities as the building blocks for constructing an anti-VEGF-A/anti-PDGF-BB DVD-Ig molecule; the Tm value of the highest peak in the DSC thermograms for the parental anti-VEGF-A mAb selected was 72°C and Tm value of the highest peak in the DSC thermograms for the parental anti-PDGF-BB mAb selected was 87°C. The resulting DVD-Ig, ABBV642, demonstrated good thermal stability properties with the midpoint temperature of the first transition of unfolding at 62°C.

ABBV642 potently binds and neutralizes all active VEGF-A isoforms and PDGF-BB with appropriate species cross-reactivity for efficacy and safety studies

ABBV642 is a humanized DVD-Ig molecule against human VEGF-A and human PDGF-BB constructed using a humanized rat anti-VEGF-A mAb and a humanized rat anti-PDGF-BB mAb generated using Aldveron cDNA immunization technology. The rat mAbs were humanized using a computer-aided high throughput humanization program developed at AbbVie. The anti-PDGF-BB mAb was further affinity matured using yeast display technology. A kinetic analysis of ABBV642 binding to VEGF-A species and PDGF-BB species were quantitatively characterized using surface plasmon resonance (SPR)

technology. ABBV642 binds human VEGF-A165 at an affinity K_D of 65 pM (on-rate ka = 5.2E+05 $M^{-1}s^{-1}$ and off-rate k_d = 3.4E-5 s^{-1}), and human PDGF-BB at an affinity of less than 5.2 pM (on-rate ka $\geq$ 1.0E+07 $M^{-1}s^{-1}$ and off-rate k_d = 5.2E-5 s^{-1}). A competition ELISA was performed to evaluate the ability of ABBV642 to block ligand-receptor interaction. ABBV642 potently blocks VEGF/VEGFR2 interaction at 71 pM (Fig. 3A) and blocks PDGF-BB/PDGFRβ interaction at 90 pM (Fig. 3B). Cellular assays were employed to assess the potency of ABBV642 to neutralize human VEGF-A165 and human PDGF-BB. Potency to human VEGF-A165 was determined using a human microvascular endothelial cells (HMVEC) bioassay. The HMVEC cells proliferate in response to VEGF-A165 stimulation. HMVEC cells incubated in the presence of ABBV642 demonstrate decreased proliferation due to antagonist activity, producing an IC50 value of 145 pM (Fig. 3C). A second VEGF-A165-dependent bioassay was used to confirm antagonist activity. Mouse fibroblast cells stably transfected with the receptor VEGF-R2 were stimulated with VEGF-A165 in the presence of ABBV642. The results clearly demonstrated a decrease in proliferation due to antagonist activity and produced an IC50 value of 433 pM (data not shown). Potency to human PDGF-BB was determined using a NIH-3T3 bioassay. These are mouse fibroblast cells which natively express the mouse receptor PDGF-Rβ. The human PDGF-BB interacts with the mouse receptor PDGF-Rβ and will induce proliferation of the cell line. NIH-3T3 cells incubated in the presence of ABBV642 demonstrated decreased proliferation due to antagonist activity and produced an IC50 value of 45 pM (Fig. 3D).

To understand whether ABBV642 can simultaneously bind and block both VEGF and PDGF-BB or not, the neutralization potency of ABBV642 for the first ligand was measured in the presence of excess amount of the second ligand. We confirmed that the excess amount of the second ligand itself alone did not affect the assay readout for the first ligand in these assays. When pre-incubated with excess hPDGF-B, ABBV642 blocks hVEGF-A165-induced Tyr1054 signaling in VEGFR2–3T3 cells at an equivalent level compared with the parental anti-VEGF clone hBEW-9E10.1 (Fig. 4A). ABBV642, when pre-
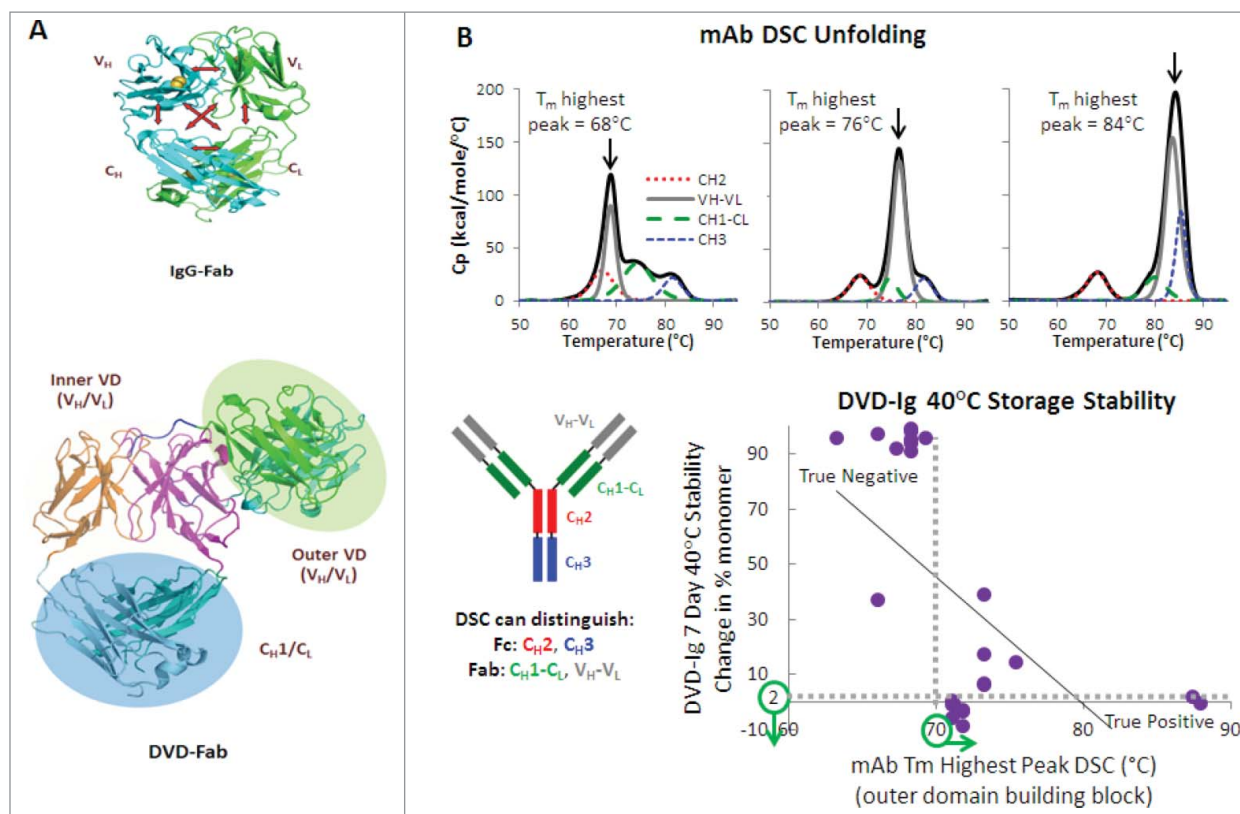
Figure 2. (A) CH1-CL interactions stabilize VH-VL in the context of a Fab of IgG molecule. This stabilization is not available for the outer domain of a DVD-Ig molecule. (B) Outer domain stability shows a correlation (r = −0.58) of statistical significance (p = 0.002) with DVD-Ig accelerated, high concentration storage stability.

incubated with excess hVEGF-A165, blocks hPDGF-BB-induced NIH-3T3 cell proliferation also at an equivalent level compared with the parental anti-PDGF-BB clone CL-33675 (Fig. 4B). These results demonstrated that binding of ABBV642 to one soluble ligand did not affect its ability to block biological activities induced by another soluble ligand.

VEGF-A mRNA undergoes alternative splicing events that generate five different homodimeric isoforms, VEGF111, VEGF121, VEGF165, VEGF189, or VEGF206. VEGF121 is a non-heparin-binding acidic protein, which is freely diffusible.[28] The longer forms, VEGF189 or VEGF206, are highly basic proteins tightly bound to extracellular heparin-containing proteoglycans.[28] VEGF165 has intermediate properties.[28] VEGF111 was also identified later as a biologically active and proteolysis-resistant splice variant of this family.[32] Pegaptanib, the first anti-VEGF-A agent approved for the treatment of exudative AMD, selectively neutralizes only VEGF165 and is less efficacious than agents that neutralize all isoforms.[33] Therefore, we selected the VEGF-A binding domain of ABBV642 that can neutralize all the active VEGF-A isoforms. The overall affinity K_Ds of ABBV642 were 65 pM for human VEGF-A 165 (on-rate $k_a = 5.2E+05M^{-1}s^{-1}$ and off-rate $k_d = 3.4E-5s^{-1}$), 230 pM for human VEGF-A 121 (on-rate $k_a = 1.8E+05 M^{-1}s^{-1}$ and off-rate $k_d = 4.1E-5s^{-1}$), and 290 pM for human VEGF-111 (on-rate $k_a = 1.5E+05M^{-1}s^{-1}$ and off-rate $k_d = 4.3E-5s^{-1}$). The neutralization of different human VEGF-A isoforms by ABBV642 was also demonstrated in cellular potency assays (data not shown). We also confirmed that ABBV642 can bind to ECM-associated PDGF-BB by immunostaining (data not shown).

Species cross-reactivity is an important consideration when assessing PK, efficacy and safety of the drug development candidates in relevant animal species, disease models, and preclinical toxicology species. ABBV642 had very weak binding to mouse and rat VEGF-A at the 500 nM concentration tested. Affinity of ABBV642 for rabbit VEGF-A was 41 pM (on-rate $k_a = 9.6E+05M^{-1}s^{-1}$ and off-rate $k_d = 4.0E-5s^{-1}$). The amino acid sequence of VEGF-A of cynomolgus monkey and human is identical. ABBV642 binds to human, cynomolgus monkey, mouse and rat PDGF-BB at high affinity, with K_D values at ≤ 5.2 pM (on-rate $k_a \geq 1.0E+07M^{-1}s^{-1}$ and off-rate $k_d = 5.2E-5s^{-1}$), 0.81 pM (on-rate $k_a \geq 1.0E+07M^{-1}s^{-1}$ and off-rate $k_d = 8.1E-6s^{-1}$), 0.36 pM (on-rate $k_a \geq 1.0E+07M^{-1}s^{-1}$ and off-rate $k_d = 3.6E-6s^{-1}$) and 2.6 pM, respectively (on-rate $k_a \geq 1.0E+07M^{-1}s^{-1}$ and off-rate $k_d = 2.6E-5s^{-1}$). The amino acid sequence of PDGF-BB in rat and rabbit is also identical.

ABBV642 inhibits endothelial tube formation and pericyte coverage in a co-culture in vitro angiogenesis assay

The abnormal new blood vessels that grow in the subretinal space in exudative AMD are made up of two cell types, endothelial cells and pericytes. The endothelial cells line the inside of the vessels and pericytes wrap around the endothelial cells. First, VEGF binds to its receptor on endothelial cells, causing them to proliferate and form new blood vessels. VEGF provides survival signals to endothelial cells and induces blood vessel permeability. Next, the endothelial cells release paracrine PDGF-BB that is retained proximally by heparin sulfate
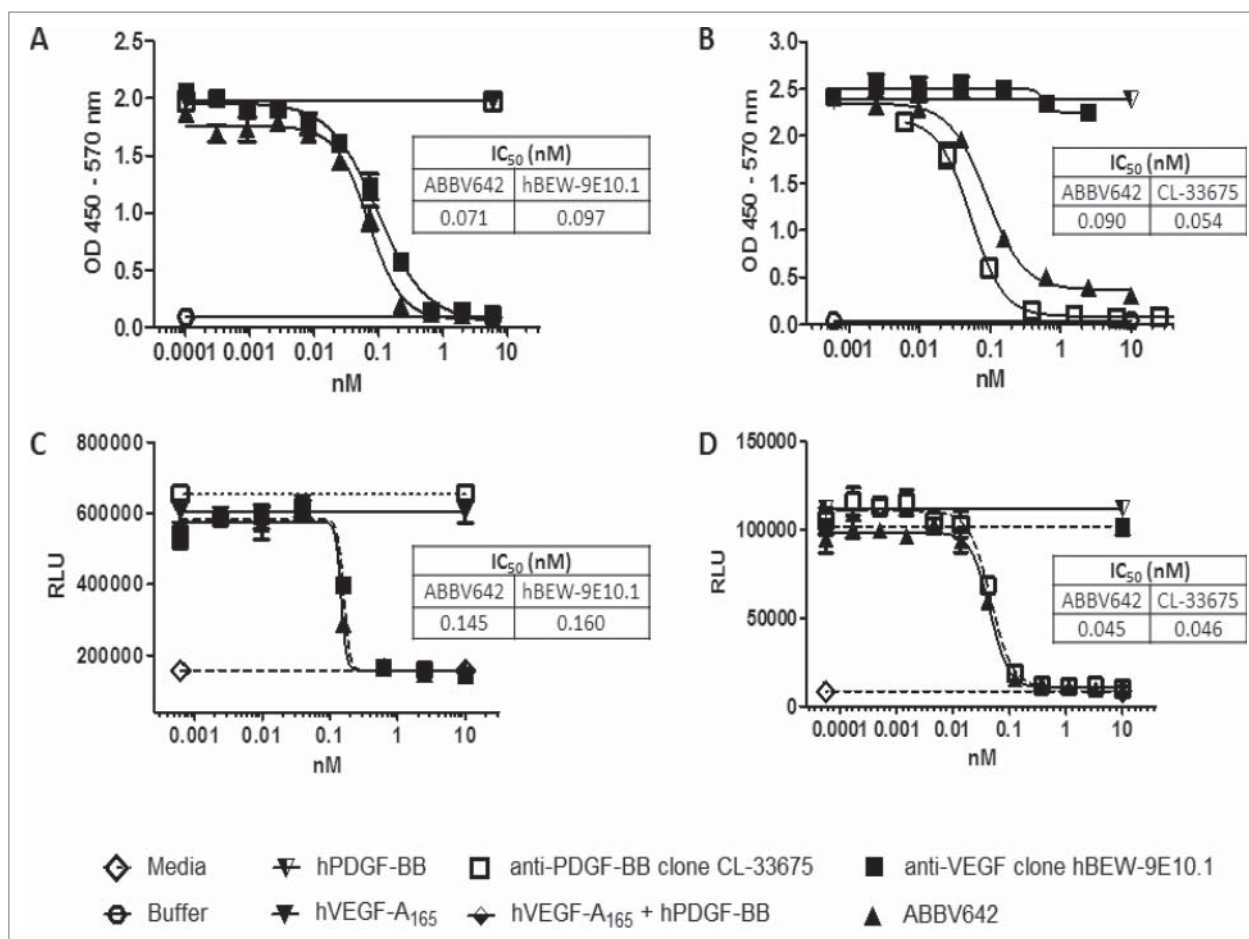
Figure 3. ABBV642 blocks ligand-receptor binding in a competition ELISA and blocks soluble ligand induced biological activities in cellular bioassays. (A) ABBV642 blocks binding of hVEGF-A165 to hVEGF-R2 in a competition ELISA. (B) ABBV642 blocks binding of hPDGF-BB to hPDGF-Rβ in a competition ELISA. (C) ABBV642 neutralizes hVEGF-A165 and blocks hVEGF-A165 induced proliferation of HMVEC-d cells. (D) ABBV642 neutralizes hPDGF-BB and blocks hPDGF-BB induced proliferation of NIH-3T3 cells.

proteoglycan to chemoattract PDGF receptor-B (PDGFR-β) expressing pericytes. The recognition of the proximally retained PDGF-BB by the pericyte-bound PDGFR-β initiates the proliferation and migration of the pericytes along the growing neovascularization.[27] The critical role of PDGF-BB/PDGFR-β interaction for pericyte recruitment and capillary maturation

has been demonstrated through gene knockout,[34] ectopic delivery of competing PDGF-BB,[35] blocking the PDGF-BB/PDGFR-β interaction by external agents,[18] or deletion of the PDGF-BB heparin sulfate proteoglycans binding motif.[36] Established subretinal vessels may have sufficient pericyte coverage to be resistant to anti-VEGF monotherapy.[18] Pericytes also produce
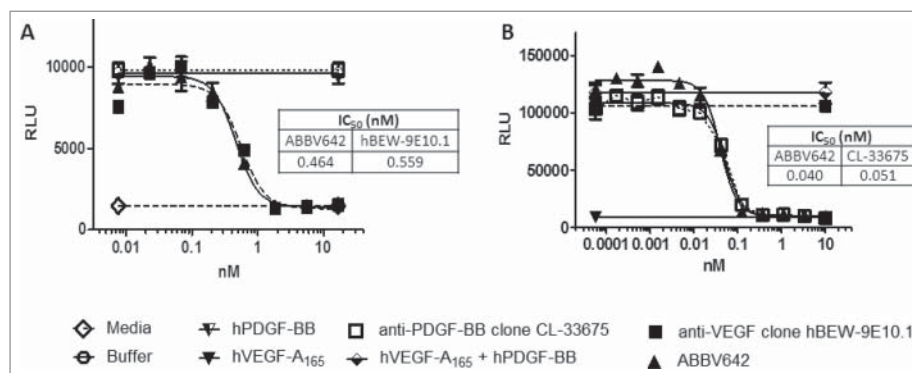

Figure 4. Binding of ABBV642 to one soluble ligand did not affect its ability to block another soluble ligand induced biological activities. (A) ABBV642, when pre-incubated with excess hPDGF-B, blocks hVEGF-A165-induced Tyr1054 signaling in VEGFR2–3T3 cells at the equivalent level as parental anti-VEGF clone hBEW-9E10.1 does. (B) ABBV642, when pre-incubated with excess hVEGF-A165, blocks hPDGF-BB-induced NIH-3T3 cell proliferation at the equivalent level as parental anti-PDGF-BB clone CL-33675 does.

VEGF to promote survival of endothelial cells. Therefore, stripping of pericytes combined with anti-VEGF therapy may lead to regression of neovascularization and improved visual outcomes.

We evaluated anti-VEGF-A mAb, anti-PDGF-BB mAb and ABBV642 for their ability to interfere with endothelial tube formation and pericyte coverage in a human umbilical vein endothelial cell (HUVEC) and human mesenchymal stem cell (MSC) co-culture in vitro angiogenesis assay. This is a semi-quantitative assay mainly for demonstrating anti-angiogenesis mechanism. Tube formation and pericyte coverage were observed with no treatment or isotype control DVD-Ig treatment (Fig. 5A-a and 5A-b). Addition of the anti-VEGF-A mAb inhibited the formation of new sprouts, but had little effect on pericyte coverage (Fig. 5A-c). Addition of anti-PDGF-BB mAb had no effect on endothelial sprouting, but reduced pericyte coverage (Fig. 5A-d). Addition of the ABBV642 or a combination of anti-VEGF-A and anti-PDGF-BB mAb reduced tube
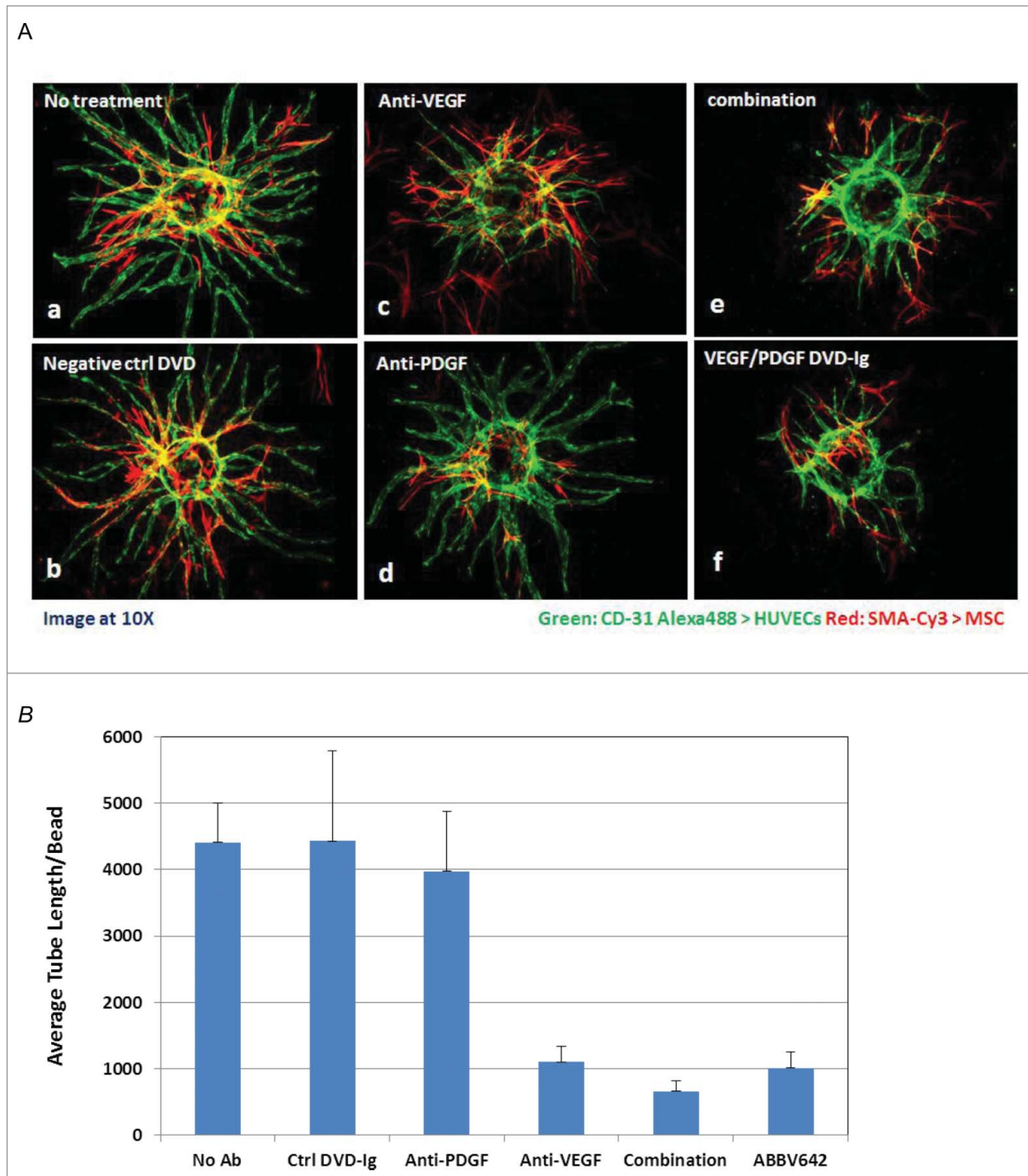
Figure 5. ABBV642 potently inhibits tube formation in a HUVEC/hMSC co-culture sprouting assay. (A) Representative images demonstrate reduced tube formation and/or pericyte coverage by various treatment (B) Total tube length from one bead was measured by Image J and average of 5 to 10 beads were plotted for each treatment with standard deviation (mean ± SD).

number and length and pericyte coverage (Fig. 5A-e and 5A-f). Semi-quantitative measurement of tube length was done by Image-J software[37] and data was analyzed using Excel and presented as mean (± SD) (Fig. 5B). These results confirm that ABBV642 suppresses both VEGF and PDGF-BB activities in an in vitro angiogenesis assay.

Systemic and ocular PK profile of ABBV642 in preclinical animals

ABBV642 has a H435A mutation in its Fc region and has no significant binding to human, cynomolgus, mouse, rat or rabbit FcRn (data not shown). Single dose intravenous (IV) PK studies were run in humanized FcRn mice (B6.Cg-FcRn-276) to compare PK profiles of ABBV642 to PK profiles of a tool DVD-Ig molecule engineered with the same Fc mutant (H435A) and a tool DVD-Ig molecule with the wild type Fc region. After a single 5 mg/kg IV injection of ABBV642 to male B6.Cg-FcRn-276 mice, serum clearance

was rapid, with measurable concentrations observed at only the 1 and 24 hour time points (Fig. 5A). The half-life of ABBV642 could not be calculated due to the paucity of measurable data points. As the controls, the half-lives of tool DVD-Ig molecules constructed with Fc H435A mutant (PR-1565689) or wild type Fc (PR-1565009), dosed at 6.7 mg/kg, are 14 and 67 hours, respectively (Fig. 6A). PK parameters are presented in Table 1. The net exposure of ABBV642 in systemic circulation for the intended route of intravitreal administration is the result of diffusion of the drug from ocular space into systemic circulation and its clearance from systemic circulation. The FcRn null mutation was reported to not have a significant effect on vitreous exposure, but to significantly reduce serum exposure following a single intravitreal administration compared with similar IgG with a wild type Fc region.[23] ABBV642 with the FcRn null mutation is therefore expected to have reduced persistence in circulation in human blood when compared with the same molecule with a wild type Fc region.
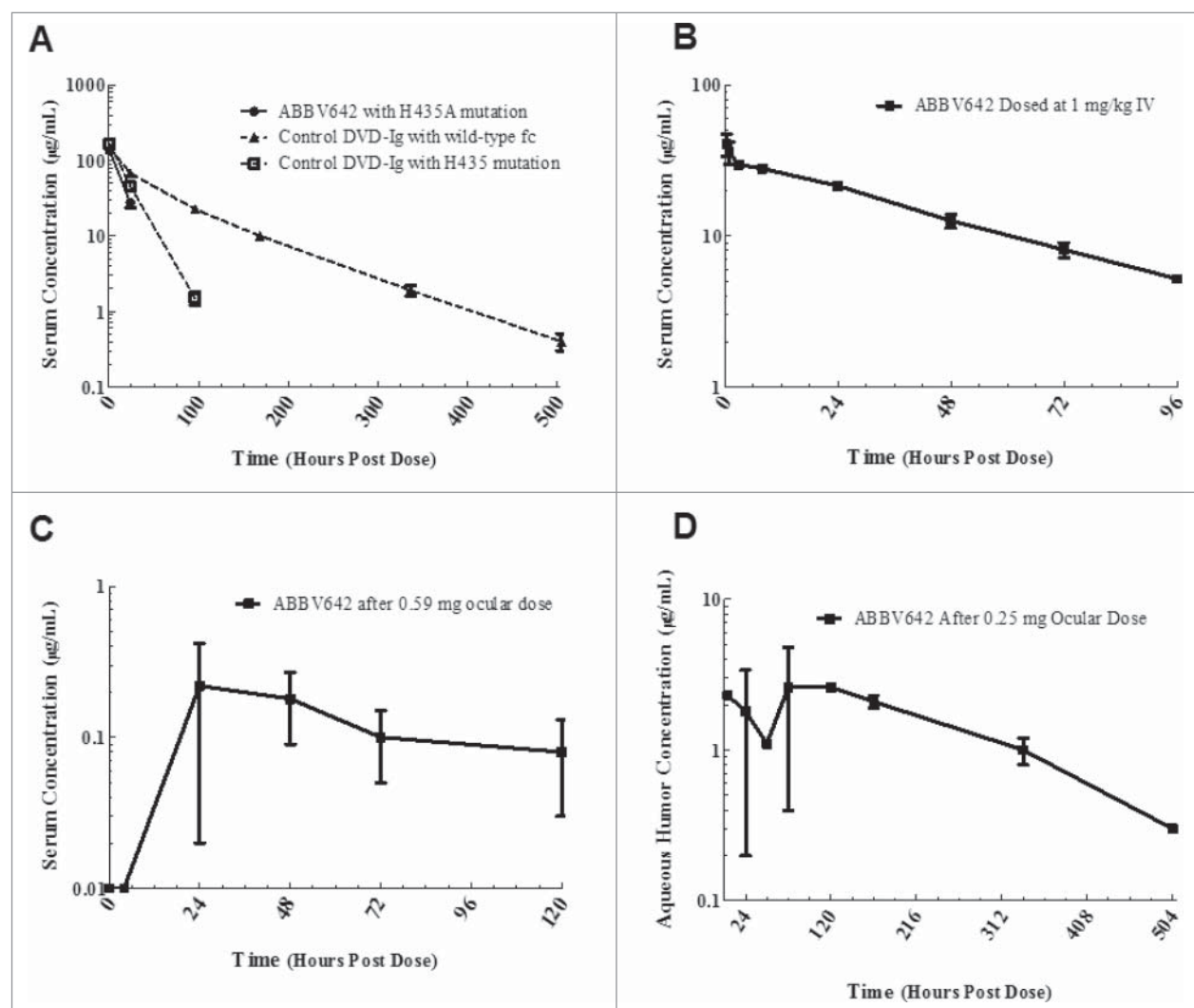
Figure 6. Systemic and ocular PK profile of ABBV642 in preclinical animals. (A) Mean (± SD) serum concentrations of ABBV642 with H435A mutation (solid circle), a control DVD-Ig with H435A mutation (open square) and a control DVD-Ig with wild-type Fc (solid triangle) following a single 5 or 6.7 mg/kg intravenous dose in male B6.Cg-FcRn-276 mice. (B) Mean (± SEM) serum concentrations of ABBV642 after a 1 mg/kg intravenous dose in New Zealand White rabbits. (C) Mean (± SEM) serum concentrations of ABBV642 after a 0.59 mg ocular dose in New Zealand White rabbits. (D) Mean (± SEM) aqueous humor concentrations of ABBV642 after a 0.25 mg ocular dose in New Zealand White rabbits.

Table 1. Pharmacokinetic parameters of three DVD-Ig molecules with or without FcRn null mutation after single dose intravenous (IV) administration in humanized FcRn (B6.Cg-FcRn-276) mice.

Compound	FcRn Binding	AUC (μg^*h/mL)	AUC/Dose (μg^*h/mL)/(mg/kg)	Cl (mL/h/kg)	$t_{1/2}$ (hours)
ABBV642	Null	1860	372	2.6	NC
PR-1565689	Null	4340	648	1.6	14
PR-1565009	Full	8280	1240	0.8	67

The PK profile of ABBV642 was also assessed following a single 1 mg/kg IV dose in New Zealand White rabbits. The mean clearance after the single ABBV642 IV administration was 0.58 mL/hr/kg, the mean volume of distribution at steady-state was 29.1 mL/kg, and the harmonic mean of the terminal half-life was 36 hours. Both animals displayed similar PK profiles, with measurable exposure lost after 4 d (Fig. 6B). The exposure, expressed as mean AUC_{0-96h}/D, was 1732 $\mu g \bullet hr$/mL.

Serum levels of ABBV642 after ocular dosing were monitored in four animals receiving a 590 μg dose to one eye (~0.2 mg/kg). In all animals dosed, serum exposure rose after a delayed systemic absorption from the eye before dropping below measurable levels after 5 d. Exposure, as measured by AUC_{0-120h} was low and variable, ranging from 11 to 22 $\mu g \bullet hr$/mL (Fig. 6C). The dose normalized systemic exposure after ocular dosing was ~4% of that seen after an intravenous dose.

Ocular levels of ABBV642 after ocular dosing were monitored in four animals, split into two groups of two, each receiving a 250 μg dose to one eye (~0.1 mg/kg). Ocular exposure, as monitored by aqueous humor concentration, was variable following diffusion of drug through the unstirred ocular compartment (Fig. 6D). Within the limits of the high variability, the estimated composite ocular half-life and AUC_{0-504} were 111 hours and 770 $\mu g \bullet hr$/mL, respectively. Concentrations of ABBV642 in both aqueous and vitreous humor were quantitated in terminal sample taken on Day 7 and Day 21. The ratio of vitreous concentration to aqueous concentration of ABBV642 was quite consistent across all samples and averaged 22:1 (range of 18–24:1), indicating that aqueous humor concentrations are a good surrogate for vitreous exposure. This result is consistent with a previous report.[23]
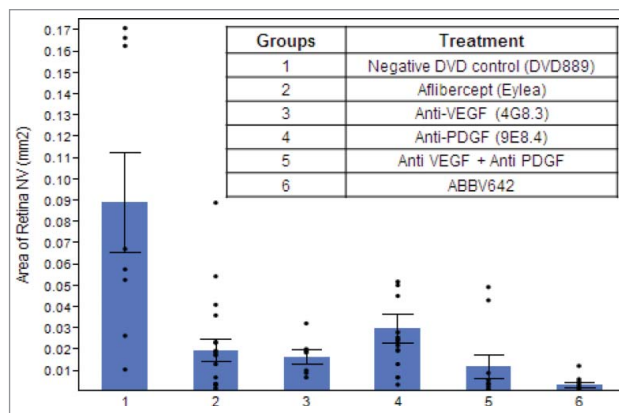
ABBV642 significantly decreased subretinal neovascularization in rho/VEGF-A transgenic mouse model

Because ABBV642 does not bind to rodent VEGF-A, we used two transgenic mouse models in which human VEGF-A165 is expressed, resulting in subretinal neovascularization, to assess the efficacy of ABBV642. Transgenic mice in which the rhodopsin promoter drives expression of human VEGF-A165 in photoreceptors (Rho-VEGF-A mice) have onset of VEGF-A expression at P7. Starting at P10, mice develop sprouts of neovascularization from the deep capillary bed of the retina that grow through the photoreceptor layer and form an extensive network of new vessels in the subretinal space.[4] Since the new vessels originate from retinal capillaries and not choroidal vessels, it is technically a model of retinal angiomatous proliferation (RAP, also known as type 3 choroidal neovascularization), which occurs in roughly 30% of patients with neovascular AMD. The positive control for these studies was aflibercept, a recombinant VEGF-neutralizing protein that is currently

widely used for standard care of exudative AMD. The concentration of aflibercept injected into human eyes is 2 mg/ml. Intraocular injection of 1 μl of the 2 mg/ml clinical concentration, which is 0.32 μmoles of aflibercept, was done and an injection of 0.32 μmoles of all other agents was done for comparison. The DVD-Ig control group had significantly greater mean area of neovascularization per retina compared with all other groups (ANOVA with Dunnett correction p < 0.0001). The mean area of neovascularization per retina was significantly less in ABBV642-treated eyes than those treated with aflibercept (Tukey HSD test, p = 0.0031). The mean area of neovascularization in the ABBV642 group was numerically less, but not significantly different from the combination of a potency matched anti-VEGF mAb and an anti-PDGF mAb (Fig. 7).

ABBV642 significantly prevented retinal detachment in Tet-opsin-VEGF double transgenic mouse model

Double transgenic mice with doxycycline (Dox)-inducible expression of human VEGF-A165 in photoreceptors express 10-fold higher levels of VEGF than Rho-VEGF transgenic mice and develop severe neovascularization and exudative retinal detachment 3 d after initiation of Dox.[38] Test agents (0.32 μmoles) were injected in one eye, Dox treatment was begun, and after 4 d retinal fundus photographs were scored using the grading scale as described in the method section. In brief, 0 = no retinal detachment (NRD), 1 = partial retinal detachment (PRD), 2 = total retinal detachment (TRD) (Fig. 8A, B and C). In 5 eyes injected with anti-VEGF-A mAb, there were no retinal detachments preventing assessment of

Figure 7. ABBV-642 significantly decreased subretinal neovascularization in Rho/VEGF-A transgenic mouse model. Area of subretinal neovascularization (NV) per retina 7 d after intraocular injection of 0.32μmoles of listed agents in Rho/VEGF-A transgenic mice was measured. The area of NV per retina was significantly less in eyes injected with ABBV642 compared with those injected with aflibercept (p = 0.0031 by Tukey HSD test).
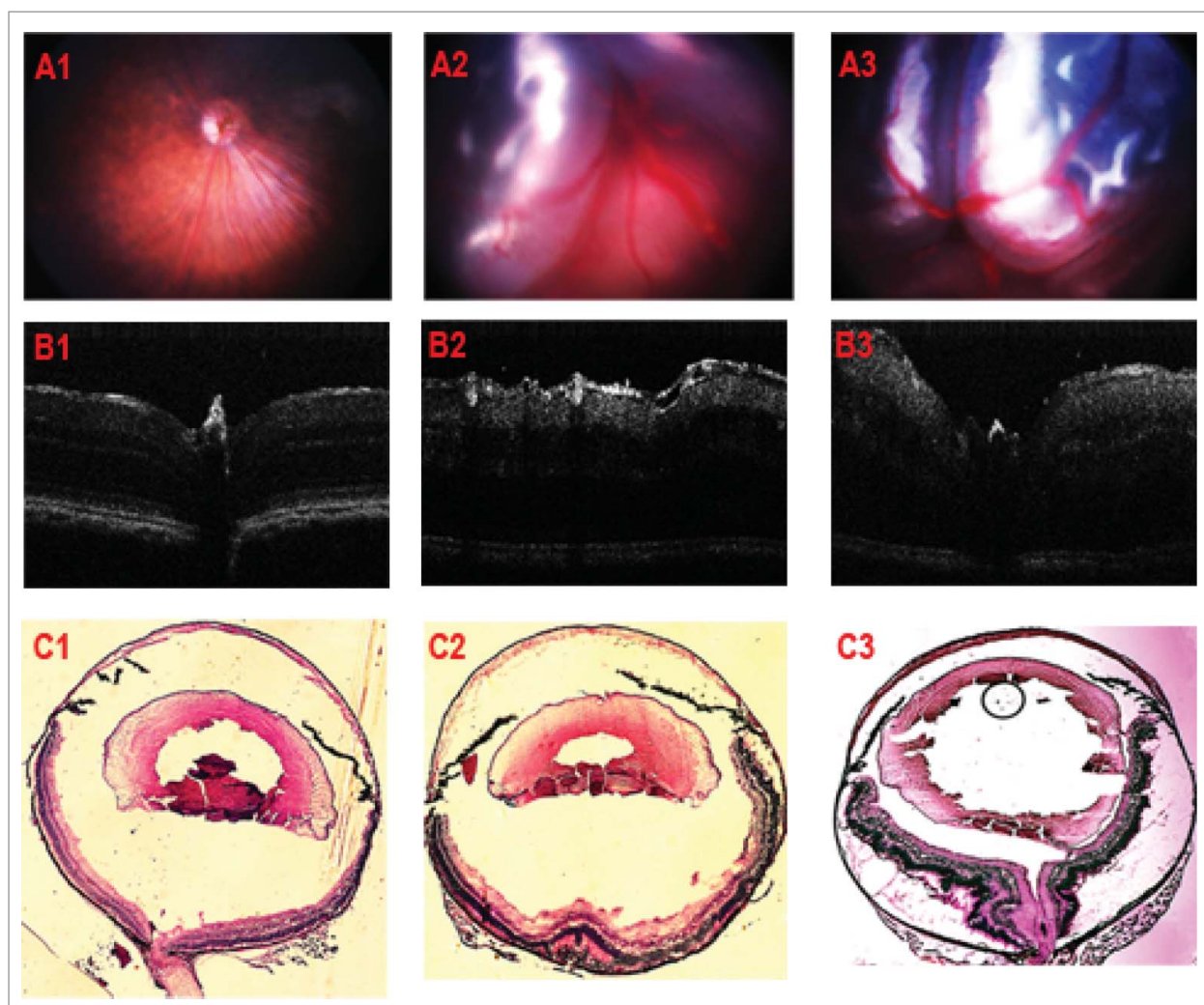
Figure 8. Typical images of the simplified RD grading in tet-opsin/huVEGF-A double transgenic mice. Fundus images with A1, A2, A3 representing NRD, PRD, TRD respectively; OCT images with B1, B2, B3 representing NRD, PRD, TRD respectively; Ocular cryo-section with H&E stain, C1, C2, C3 represent NRD, PRD, TRD respectively.

improved activity by addition of anti-PDGF-BB mAb in the combination group. However, only 1 of 11 eyes (9%) injected with ABBV642 had a retinal detachment compared with 4 of 8 (50%) of eyes injected with aflibercept, and 7 of 9 eyes (78%) injected with control IgG (Table 2). These data suggest that ABBV642 strongly suppresses exudative retinal detachment in this particularly severe disease model.

Discussion

AMD is a complex disease in which a subgroup of patients with exudative AMD has stabilization of HIF-1 in photoreceptors and RPE cells, resulting in upregulation of VEGF and other vasoactive proteins. PDGF-BB has been implicated as a second contributor to subretinal neovascularization because PDGF-BB antagonists cause modest suppression in a mouse model[18] and because combined suppression of VEGF and PDGF-BB causes greater neovascularization suppression than either alone.[17,18] Here, we report the development of a new biologic that addresses many of the problems of current treatments for exudative AMD. We developed a novel dual variable domain immunoglobulin molecule, ABBV642, which specifically and potently neutralizes all isoforms of VEGF-A and both soluble and ECM-bound PDGF-BB. In an in vitro angiogenesis model,

Table 2. The efficacy of test agents in Tet/opsin/VEGF double transgenic mice[*].

Grade	IgG control	Anti-VEGF mAb	Anti-PDGF mAb	Anti-VEGF + Anti-PDGF	ABBV642	Aflibercept
0 (NRD)	2	5	2	7	10	4
1 (PRD)	1	0	2	1	0	3
2 (TRD)	6	0	3	0	1	1
Total eyes	9	5	7	8	11	8

[*]Intraocular injection (one per mouse) with 0.32 μmoles of one of the above listed agents was followed by daily subcutaneous injections of 500mg/kg of doxycycline. On day 4 after injections fundus photographs were graded for exudative retinal detachment.

ABBV642 suppressed both endothelial tube formation, a VEGF-stimulated activity, and pericyte coverage, a PDGF-BB-stimulated activity. ABBV642 does not cross-react with mouse VEGF, and therefore it was tested in two transgenic mouse models in which human VEGF165 is expressed in photoreceptors: Rho/VEGF and Tet/opsin/VEGF mice. In Rho/VEGF mice, expression of VEGF in photoreceptors begins at P7 and persists thereafter, resulting in progressively worsening subretinal neovascularization. Intraocular injection of 0.32 μmoles of ABBV642 caused greater suppression of subretinal neovascularization than injection of 0.32 μmoles of aflibercept. In a model with high expression of VEGF in photoreceptors, 9% of eyes injected with 0.32 μmoles ABBV642 developed exudative retinal detachment compared with 50% of eyes injected with 0.32 μmoles of aflibercept. These data suggest that ABBV642 is highly efficacious in mouse models predictive of effects in exudative AMD, similar to what is observed with combination treatment of separate anti-VEGF and anti-PDGF antagonists.[18]

Enhancing short-term outcomes is important, but the ultimate goal is to provide sustained long-term benefits. ABBV642 was engineered to potentially increase durability of activity in the eye to maximize long-term benefits. This was done by making ABBV642 a 200 kDa full-length IgG, i.e., with a molecular weight over 50 kDa larger than a canonical IgG antibody and over 100 kDa larger than aflibercept. After an injection of 250 μg of ABBV642 in rabbit eyes, aqueous levels decreased with a half-life of 4.6 days, which compares favorably to the aqueous half-life of 2 d of aflibercept in rabbit eyes[21] and is similar to a published vitreal half-life of bevacizumab of 4.3 d.[39] A previous study reported that the difference in molecular weight of 50 to 150 kDa only had a small effect on the vitreous half-life, which ranged from 3.2 to 5.2 d.[23] Further study may be required to understand the effect of larger molecular size on ocular PK and how this is compared with other biological therapies for the treatment of wet AMD. The additive effect of combined suppression of VEGF and PDGF-BB in a single bispecific agent may also reduce the frequency of injections. Once dosed into the ocular compartment, drug is cleared from the eye into the systemic circulation by various mechanisms and can be persistent.[23,40] The kinetics of net exposure of drug in systemic circulation for the intended route of intravitreal administration is the result of diffusion of the drug from ocular space into systemic circulation and its clearance from systemic circulation.[23] After ABBV642 exits the eye, rapid elimination from the circulation is desired to reduce systemic effects. ABBV642 was engineered to minimize FcRn binding with an H435A mutation in the Fc region of the molecule for rapid clearance in systemic circulation. After IV dosing, we observed that ABBV642 was eliminated from the circulation more rapidly than a wild-type IgG molecule with normal FcRn binding in humanized FcRn mice. To further insure against potential adverse effects, L234A, L235A mutations in the low hinge Fc region were introduced to attenuate binding to FcγRI, FcγRII and C1q molecules, thus reducing the potential for ADCC and CDC activity.

Exudative AMD is a major public health problem. Intraocular injection of specific VEGF-neutralizing proteins has provided substantial short-term visual benefits in many but not all patients. However, most benefits are lost over time, often due to development of subretinal fibrosis, and PDGF-BB is an important stimulus for fibrosis in the eye.[12-16] Loss of visual acuity gain benefit over time has also been linked to an inability to maintain the recommended frequency of injections needed to maintain disease quiescence.[41] ABBV642 addresses these issues by suppressing VEGF and PDGF-BB with a single injection and prolonging residence time in the vitreous cavity to reduce injection frequency, while at the same time minimizing systemic exposure. The translation of these effects in patients with exudative AMD remains to be tested in clinical studies.

Materials and methods

Molecular cloning, protein expression and purification

ABBV642 is a humanized DVD-Ig molecule that targets human VEGF-A and human PDGF-BB. Parental mAbs for the DVD-Ig molecule were generated using rat hybridoma technology at Aldevron (Madison, WI), and hybridoma supernatants were subsequently screened for activity at AbbVie Bioresearch Center (Worcester, MA). Antibody heavy and light chain variable regions (VH and VL) of the selected hybridomas were cloned and expressed as chimeric antibodies, and then further humanized using computer-aided high throughput humanization design software developed at AbbVie. The affinity of the anti-PDGF humanized mAb was further improved through affinity maturation using yeast display technology. DNA for the DVD-Ig molecule was generated using overlapping PCR with the parent mAb DNA as template DNA and the primers. The first-round PCR used the parent mAb DNA as template and the appropriate vector and mAb-linker primers using KOD Hot Start DNA Polymerase (EMD Millipore 71086). The PCR reaction was purified using Qiagen Qiaquick PCR Purification Kit (28104 or 963141). The first-round PCRs were used as the DNA template with the appropriate vector primers. The second-round PCR was purified using Qiagen PCR Purification Kit (28104 or 963141), the DNA concentration was determined by nanodrop reading and multiple PCRs were pooled for digest. PCR products and vectors were digested with XbaI and SalI for HCs or XbaI and BsiWI for LCs. The HC vector used for cloning was pHybE-hCg1mut (L234A, L235A, H435A) and the LC vector was pHybE-hCKappa. Digested DNA was run on agarose gel, the appropriate sized band was extracted and Qiagen Gel Extraction Kit (28704) was used to clean the DNA. PCR products were cloned into vectors using T4 DNA Ligase (NEB M0202S) and ligation reaction was transformed into DH5α cells. Colonies were sequenced to identify vectors with correct DNA sequence, and then E.coli were grown for DNA Maxiprep using Invitrogen BenchPro (MC2001).

ABBV642 was transiently transfected into 500 mls of Expi293 suspension cell cultures using the ExpiFectamine kit (LifeTechnologies A14524) with a ratio of 60% to 40% light to heavy chain construct. Supernatants were harvested after six days in shaking flasks, centrifuged to pellet cells, and filtered through 0.22 μm filters to separate IgG from culture contaminates. All were purified via gravity flow using 1–2 ml of rProteinA sepharose fast flow beads (GE Healthcare, 17–1279–04) over poly prep chromatography columns (Bio Rad, 731–1550). Once supernatants had passed through the columns, the beads were washed with 10 column

volumes of binding buffer, and IgG was eluted with Immunopure IgG elution buffer (Pierce, 185 1520) and collected in 1 ml aliquots. Fractions containing DVD-Ig were pooled and dialyzed into 15 mM histidine pH 6 (also known as UBC) overnight at 4°C. DVD-Ig protein was analyzed for protein concentration using NanoDrop (Thermo Fisher Scientific, Waltham, MA), purification yield, monomer percentage by size exclusion chromatography and protein identity was verified using mass spectrometry.

Affinity measurement of ABBV642

Goat antibodies specific to the Fc region of human IgG (Jackson ImmunoResearch Laboratories, Code# 109–001–008) were used to capture ABBV642 and parental mAbs. They were covalently linked to the carboxy methyl dextran matrix of the CM5 biosensor chip for VEGF-A and CM4 chip for PDGF-BB via free amine groups using an amine coupling kit (GE Healthcare Life Sciences) and the immobilization wizard option of the Biacore instruments controlling software. Carboxyl groups of the dextran matrix on the chip were activated with 100 mM N-hydroxysuccinimide, (NHS) and 400 mM 1-ethyl-3-(3-dimethylaminopropyl) carbodiimide (EDC). Goat anti-human IgG Fc (25 μg/mL), diluted in 10 mM sodium acetate, pH 4.5, was injected across the activated surface. Once the level of binding response reached the desired value, unreacted groups were deactivated by injection of 1 M ethanolamine. Approximately 5000RU of goat anti-human IgG Fc were immobilized on the chip surface on flow cells 2, 3 and 4. A modified CM surface with conjugated goat IgG antibodies in flowcell 1 was used as a reference surface. HBS-EP with added 0.1 mg/ml bovine serum albumin (BSA) served as a running buffer. ABBV642 and parental mAbs diluted to 1 μg/mL were injected over the goat anti-human IgG Fc surface on flow cells 2, 3 and 4, at a flow rate of 50 μL/min, to achieve capture level of ~70–200 RU. The net difference in the baseline signal and the signal after the completion of the antibody injection was taken to represent the amount of bound DVD-Ig molecules or mAbs. Each antigen binding experiment consisted of antigen association and antigen dissociation phases. Aliquots of recombinant antigens were injected at different concentrations at a flow rate of 50 μL/min for 5 minutes over the captured immunoglobulins and the reference surface to ascertain association rates.

Recombinant VEGF-A was tested at concentrations of 0, 0.08, 0.4, 2, 10, 50, 250 nM (in some cases where on-rate was too fast, 250 nM concentration was removed to improve fit). Recombinant PDGF-BB species were tested at concentrations of 0, 0.0032, 0.016, 0.08, 0.4, 2, 10 nM. Dissociation phase consisted of continuous flow of buffer at 50 μL/min at two dissociation times (30 min for 50 and 10 nM human and rabbit VEGFA and 10 and 2 nM PDGF-BB and 10 min for lower concentrations of these antigens). The instrument response is measured in RU, and is proportionate to the mass of bound VEGFA and PDGF-BB species. Immobilized surfaces were regenerated with 25 μL injections of 10 mM glycine (pH 1.5) at a flow rate of 50 μL/min before the injection of the next sample. Each interaction of DVD-Ig molecules and mAbs with VEGF-A and PDGF-BB antigen species was run as n = 2. The reference surface response was subtracted from the reaction surface data in order to eliminate change in the refractive index and injection noise.

The association rate constants (k_a, units of $M^{-1}s^{-1}$) were derived by kinetic binding measurements at several antigen concentrations. Dissociation rate constants (k_d, s^{-1}) were determined by measuring changes in the amount of antigen bound to DVD-Ig molecules and mAbs over time after the association phase was complete. Association and dissociation rate constants were calculated by the instrument appropriate evaluation software based on the values extracted from the data using global fit analysis (allowing identical values for each parameter in the data set, except for Rmax that was set local due to variation in DVD-Ig molecules and mAbs capture level). The value of 1×10^7 $M^{-1}s^{-1}$ was used as an instrument detection limit for the on rate. In cases, where the limit of detection was exceeded, a qualifier of "$\geq 1 \times 10^7$" was used for the on rate and apparent overall average dissociation constant (K_D) was expressed as $K_D \leq k_d / 1 \times 10^7$. The goodness-of-fit between the 1:1 model fitted curve and the experimental data was expressed by the evaluation software as Chi2.

Blockade of ligand-receptor interaction by ABBV642

hVEGF-A165 / hVEGF-R2-Fc competition ELISA

To examine the ability of ABBV642 to block the interaction of hVEGF-A165 with hVEGF-R2 (KDR/Flk-1) receptor, a competition ELISA was performed. 96-well Costar high binding plates (Corning Cat# 3369) were coated with 0.5 μg/mL recombinant human VEGF-R2-Fc (R&D Systems cat#357-K_D 50 μL/well in D-PBS), shaken for 2 hours at 25°C and stored overnight at 4°C. Plates were washed with wash buffer (TBS, 0.05% Tween-20) and blocked with Superblock blocking buffer (Thermo Scientific, Cat# 37535). During the blocking step, the monoclonal antibodies anti-VEGF clone hBEW-9E10.1 and DVD-Ig molecule ABBV642 were diluted in 1% Blocker BSA (Thermo Scientific cat#37525) and an eight-point titration of each sample molecule was performed. The biotinylated human VEGF-A165 (Abbvie) was diluted in 1% Blocker BSA at 35 ng/mL. The samples were added to the biotinylated human VEGF165 (17.5 ng/mL final concentration) and pre-incubated for 45 minutes at 25°C with shaking. The pre-incubated sample/ hVEGF-A165 complex was added to the coated plate at 50 μL in duplicate and incubated for 30 minutes at 25°C with shaking. Following incubation, plates were washed with wash buffer. Streptavidin-polyHRP-40 (Fitzgerald Cat# 65r-s104phrp) was diluted in assay diluent (10% Superblock containing 0.05% surfactants) and added to plates (50 μL) for 45 minutes at 25°C with shaking. Plates were washed with wash buffer and developed with the addition of Enhanced K-blue TMB substrate (Neogen, Cat# 308177). The reaction was stopped with 2 N sulfuric acid (VWR, Cat# BDH3500–1) and the absorbance was read at 450 nm – 570 nm. A decrease in observed optical density indicates the test molecule is blocking hVEGF-A165 binding to the hVEGF-R2-Fc. Data was analyzed using Softmax Pro 4.8 software and IC$_{50}$ values calculated using a sigmoidal dose response (variable slope) fit in GraphPad Prism 5.

hPDGF-BB / hPDGF-Rβ competition ELISA

To evaluate the ability of ABBV642 to block the interaction of hPDGF-BB with hPDGF-Rβ, a competition ELISA was developed and performed. 96-well Costar high binding plates

(Corning, Cat# 3369) were coated with 0.5 μg/mL recombinant human PDGF-Rβ-Fc (R&D Systems #385-PR, 50 μL/ well in D-PBS), shaken for 2 hours at 25°C and stored overnight at 4°C. Plates were washed four times with wash buffer (TBS, 0.05% Tween-20) and blocked with Superblock blocking buffer (Thermo Scientific, Cat# 37535). During the blocking step, monoclonal antibodies anti-PDGF-BB clone CL-33675 and DVD-Ig molecule ABBV642 were diluted in assay diluent (10% Superblock containing 0.05% surfactants) and an eight-point titration of each sample molecule was performed. The recombinant human PDGF-BB-biotin (CST Cat# 8912BF; labeled at AbbVie) was diluted in assay diluent at 20 ng/mL. The sample molecule titration was added to the human PDGF-BB-biotin (10 ng/mL / 3.97E-10 M final concentration) and pre-incubated for 45 minutes at 25°C with shaking. The pre-incubated sample/PDGF-BB complex was added to the coated plate at 50 μL in duplicate and incubated for 35 minutes at 25°C with shaking. Following incubation, plates were washed with wash buffer. Detection reagent Streptavidin-polyHRP-40 (Fitzgerald, Cat# 65r-s104phrp) was diluted in assay diluent and added to plates (50 μL) for 45 minutes at 25°C with shaking. Plates were washed with wash buffer and developed with the addition of Enhanced K-blue TMB substrate (Neogen, Cat# 308177). The reaction was stopped with 2 N sulfuric acid (VWR, Cat# BDH3500–1) and the absorbance was read at 450 nm – 570 nm. A decrease in observed optical density indicates the test molecule is blocking hPDGF-BB binding to the human PDGF-Rβ-Fc. Data was analyzed using Softmax Pro 4.8 software and IC_{50} values calculated using a sigmoidal dose response (variable slope) fit in GraphPad Prism 5.

Evaluation of potency of ABBV642

Human microvascular endothelial Cell (HMVEC) proliferation assay

Human microvascular endothelial cells (Lonza, cat#CC-2516) were maintained in EBM-2 (Lonza cat#CC3156) supplemented with EGM-2V singlequots (Lonza cat#3202). Day of assay, the cells (passage 2–7) were trypsinized, washed in D-PBS and resuspended at 1E5 cells/mL in assay media (M199, 2 mM L-glutamine, 100 units/mL penicillin/ 100 μg/mL streptomycin, 10 mM HEPES and 10% FBS). Cells were plated at 5,000 cells on 96-well gelatin coated plates (BD Biocoat cat#354689) and incubated at 37°C, 5% CO_2. The anti-VEGF-A monoclonal antibodies, benchmark compounds or DVD-Ig molecules were serially diluted in assay media and pre-incubated with recombinant human VEGFA165 (1.3E-10 M final concentration) for 1 hour at 25°C with gentle shaking. The pre-incubated samples were added to the cells and plates were incubated at 37°C, 5% CO_2 for 72 hours. Cell survival/proliferation was measured indirectly by assessing ATP levels using the CellTiter-Glo Luminescent Cell Viability Assay kit (Promega, Madison, WI). A decrease in observed signal indicates the test molecule is neutralizing the hVEGF165 induced proliferation. IC_{50} values were calculated using a sigmoidal dose response (variable slope) fit in GraphPad Prism 5.

VEGFR2–3T3 proliferation assay

Stably transfected VEGFR2–3T3 cells were trypsinized, washed in D-PBS and resuspended at 8.5E4 cells/mL in assay media (DMEM, 2 mM L-glutamine, 100 units/mL penicillin/ 100 μg/mL streptomycin, 0.1% MEM non-essential amino acids, 1 mM sodium pyruvate and 0.1% BSA). Cells were plated at 4,250 cells / well on black 96-well plates and incubated for 24 hours at 37°C, 5% CO_2. The following day, anti-VEGF-A monoclonal antibodies, benchmark compounds or DVD-Ig molecules were serially diluted in assay media and pre-incubated with recombinant VEGF-A165 (1.04E-9 M final concentration) for 1 hour at 25°C with gentle shaking. The pre-incubated samples were then added to the cells and plates were incubated at 37°C, 5% CO_2 for 72 hours. Cell survival/proliferation was measured indirectly by assessing ATP levels using an ATPlite kit (Perkin Elmer, Waltham, MA). A decrease in observed signal indicates the test molecule is neutralizing the VEGF-A165 induced proliferation. IC_{50} values were calculated using a sigmoidal dose response (variable slope) fit in GraphPad Prism 5. This assay format was also used to evaluate species cross-reactivity to rabbit VEGF-A165 and human isoforms VEGF-A121 and VEGF-A111.

NIH-3T3 proliferation assay

NIH-3T3 cells (ATCC, cat#CRL-1658) were trypsinized, washed in D-PBS and resuspended at 4.5E4 cells/mL in assay media (DMEM, 2 mM L-glutamine, 100 units/mL penicillin/ 100 μg/mL streptomycin, 0.1% MEM non-essential amino acids, 1 mM sodium pyruvate and 0.1% BSA). Cells were plated at 2,250 cells / well on black 96-well plates and incubated for 5 hours at 37°C, 5% CO_2. During cell incubation, anti-PDGF-BB monoclonal antibodies, benchmark compounds or DVD-Ig molecules were serially diluted and pre-incubated with recombinant human PDGF-BB (CST, cat#8912BF) (6.63E-11 M final concentration) for 1 hour at 25°C with gentle shaking. The pre-incubated samples were then added to the cells and plates were incubated at 37°C, 5% CO_2 for 44 hours. Cell survival/proliferation was measured indirectly by assessing ATP levels using a CellTiter-Glo Luminescent Cell Viability Assay kit (Promega, Madison, WI). A decrease in observed signal indicates the test molecule is neutralizing the human PDGF-BB induced proliferation. IC_{50} values were calculated using a sigmoidal dose response (variable slope) fit in GraphPad Prism 5. This assay format was also used to evaluate species cross-reactivity to cynomolgus, mouse, rat and rabbit PDGF-BB.

Ligand co-incubation VEGF-R2 phosphorylation assay

Stably transfected VEGFR2–3T3 cells were trypsinized, washed in D-PBS and re-suspended at 3.5E5 cells/mL in growth media (DMEM, 2 mM L-glutamine, 100 units/mL penicillin/ 100 μg/mL streptomycin, 0.1% MEM non-essential amino acids, 1 mM sodium pyruvate, 400 μg/mL geneticin and 10% FBS). Cells were plated at 3.5E4 cells/well on 96-well plates (Costar cat#3599) and incubated for 6 hours at 37°C, 5% CO_2. Cells were washed with D-PBS and incubated in starvation media (DMEM, 2mM L-glutamine, 100 units/mL penicillin/100 μg/mL streptomycin and 1 mM sodium pyruvate) for 18 hours at 37°C, 5% CO_2. The following day, the MSD anti-VEGFR2-phospho assay plate (Mesoscale VEGFR2-Tyr1054 phospho-

MSD kit, cat#K151DJD-2) was blocked with MSD Blocker-A for 1 hour at 25°C with shaking. The anti-VEGF-A monoclonal antibodies, benchmark compounds or DVD-Ig were serially diluted in growth media and pre-incubated with recombinant human PDGF-BB (3.94E-8 M) for 30 minutes at 25°C with shaking. Following the first pre-incubation step, recombinant human VEGF-A 165 (1.3E-9 M) was added to the samples and incubation was continued for 30 minutes at 25°C with shaking. Starvation media was removed and pre-incubated samples were added to cells for 8 minutes at 37°C, 5% CO2. Plates were transferred to ice where media was removed and cells washed with ice-cold D-PBS. Plates were frozen for 10 minutes at −80°C and thawed on ice. To generate lysates, ice-cold lysis buffer (CST cat#9803S) containing 1 mM phenylmethylsulfonyl fluoride (PMSF) was added to cells followed by centrifugation at 3000 rpm, 4°C for 15 minutes. Lysates were transferred to MSD plate and incubated 1 hour at 25°C with shaking. Following incubation, the MSD plate was washed with assay wash buffer. The anti-phospho-Tyr1054-IgG-sulfotag reagent was added to wells and incubated in dark for 1 hour at 25°C with shaking. Plates were washed, MSD read buffer was added to wells and plates were read on a MSD Sector Imager 6000. A decrease in observed signal indicates the test molecule is neutralizing the hVEGF-A165 mediated activation in the presence of hPDGF-BB. Data was analyzed using Graphpad Prism software and IC_{50} values calculated using a sigmoidal dose response (variable slope) fit in GraphPad Prism 5.

Ligand co-incubation NIH-3T3 proliferation assay

NIH-3T3 cells (ATCC, cat#CRL-1658) were trypsinized, washed in D-PBS and re-suspended at 5E4 cells/mL in assay media (DMEM, 2mM L-glutamine, 100 units/mL penicillin/ 100 μg/mL streptomycin, 0.1% MEM non-essential amino acids, 1 mM sodium pyruvate and 0.1% BSA). Cells were plated at 2,500 cells / well (50 μL) on black 96-well plates and incubated for 5 hours at 37°C, 5% CO_2. During cell incubation, anti-PDGF-BB monoclonal antibodies, benchmark compounds or DVD-Ig molecules were serially diluted in assay media containing human VEGF-A165 (104.2 nM). The samples were pre-incubated with recombinant PDGF-BB in assay media (6.63E-11 M final concentration) for 1 hour at 25°C with gentle shaking. The pre-incubated samples were added to the cells and plates were incubated at 37°C, 5% CO_2 for 44 hours. Cell survival/proliferation was measured indirectly by assessing ATP levels using a Cell-Titer-Glo Luminescent Cell Viability Assay kit (Promega, Madison, WI). A decrease in observed signal indicates the test molecule is neutralizing the hPDGF-BB induced proliferation in the presence of hVEGF165. Data was analyzed and IC_{50} values calculated using a sigmoidal dose response (variable slope) fit in GraphPad Prism 5.

Evaluation of anti-angiogenesis activity of ABBV642 in HUVEC/human MSC co-culture sprouting assay

Cytodex-3 beads (Sigma-Aldrich, cat# C3275) were coated with HUVEC cells (Lonza) 400 cells/bead, overnight, and then embedded (200 beads/ml) with human MSC cells (Lonza, 160 K cells/ml) in fibrin gel in tissue culture plates (1 ml/well in 12-well plate). A 1:1 mixture of fresh EGM-2 complete media (Lonza) and fibroblast (Lonza) conditioned EGM-2 media were added on top of the fibrin gel along with 2 ng/mL of recombinant human hepatocyte growth factor (Sigma, Cat#H14014)). Medium was replaced every 2–3 d until the end of the experiment (20 days). Anti-VEGF-A mAb, anti-PDGF-BB mAb, combination, ABBV642 or negative control DVD-Ig molecule were added to the culture medium at 20 nM starting from day 6 after endothelial cell sprouts and pericytes covering were formed. 14 d after addition of antagonists, cells were fixed in formalin and blocked with blocking buffer overnight at 4°C. Endothelial cells were stained with anti-CD31 (Abcam, ab32457), followed by Donkey anti Rabbit IgG-H&L (Alexa Fluor 488 Cat#: ab150073), and pericytes were stained with anti-αSMA-Cy3 (Sigma, C6198). Cells were then viewed by an inverted fluorescence microscope and 5–10 beads were captured for each treatment with 10x objective. Semi-quantitative measurement of tube length was done by Image-J software[37] and data was analyzed using Excel and presented as mean ± SD.

Characterization of systemic pharmacokinetics profile of ABBV642 in humanized FcRn mice

Studies were conducted in accordance with the AbbVie Institutional Animal Care And Use Committee (IACUC) guidelines. ABBV642 was IV administered at 5 mg/kg to male B6.Cg-FcRn-276 mice (The Jackson Laboratories, Bar Harbor, ME). Whole blood samples (20 μL of whole blood diluted into 80 μL assay buffer) were collected from mice at 1 and 24 hours, and on Days 4, 7, 10, 14 and 21. Two control DVD-Ig molecules were IV administered at 6.7 mg/kg to male B6.Cg-FcRn-276 mice. Whole blood samples (20 μL of whole blood diluted into 80 μL assay buffer) were collected from mice at 1 and 24 hours, and on Days 4, 7, 14 and 21. All samples were stored at −80°C until analysis.

Serum and blood samples were analyzed using an MSD assay employing VEGF biotin for capture and Sulfo-Tag labeled goat anti-human IgG antibody for chemiluminescent detection. The assay was performed in 1% final concentration FcRn mouse serum. Standard curve fitting and data evaluation was performed using XLfit4 software. A calibration curve was plotted from MSD luminescence units vs. theoretical standard concentrations. A four-parameter logistic model was used for curve fitting. The regression equation for the calibration curve was then used to back calculate the measured concentrations. Plates passed when at least 2/3 of the QCs were within 30% of the expected values. The linear range of the MSD assay of ABBV642 was 0.027–20 μg/mL. The lower limit of quantitation (LLOQ) was 0.027 μg/mL. The linear range of the MSD assay for both control DVD-Ig molecules was 0.020–20 μg/mL. The LLOQ was 0.020 μg/mL. Values that were below the quantitation limit (BQL) of any assay were omitted from calculations. PK parameters were calculated with Pharmacokinetics Laboratory Automation Software for Management and Analysis (PLASMA) Version 2.6.12 (SPaRCS, AbbVie) using the linear trapezoidal method, and non-compartmental analysis.

Characterization of systemic and ocular pharmacokinetics profile of ABBV642 in New Zealand White rabbits

Studies were conducted in accordance with the AbbVie IACUC guidelines. Female New Zealand White rabbits were used for both ocular and systemic PK characterization of ABBV642. The animals in these experiments were weight matched at 2.7 ± 0.1 kg. Test article was IV administered into the lateral ear vein of two animals for determination of serum PK profiles and parameters after IV injection. The dose (1 mg/kg) was administered at a dose volume of 0.5 mL/kg. Whole blood samples (0.50 μL) were collected from the medial ear artery and allowed to clot for the harvest of serum, prior to being transferred into polypropylene strip tubes. Serum samples were collected at 0.5, 1, 3, 8, 24, 48, 72, 96, 168, 336, 504, and 672 hours post dosing.

Animals (four animals) were split into two cohorts of two for determination of ocular PK. Prior to ocular injection, animals were anesthetized and their eyes were treated with analgesic drops and antiseptic. Test article was dosed into the vitreous compartment at 0.59 mg per eye with a dose volume of 0.050 mL. Only the right eye of each animal was dosed. Samples of aqueous humor were taken at 4, 24, 48, 72, 120, 168, 336 and 504 hours post dosing, with cohort 1 providing samples at 4, 48, 120 and 168 hours, and cohort 2 providing samples at 24, 72, 336 and 504 hours, post dosing. Drug levels in the eye were determined from concentrations in aqueous humor as a surrogate for the vitreous concentrations. Vitreous was harvested from each animal as a terminal sample after the last aqueous humor sample. The vitreous to aqueous concentration ratio was determined from these terminal time points.

Animals (four animals) were split into two cohorts of two and were dosed by the ocular route to provide systemic exposure of PR-1610561 after an ocular dose of 0.25 mg. Blood samples for the harvest of serum used to estimate systemic exposure after vitreous dosing were also collected at 4, 24, 48, 72, 120, and 168 hours post dosing from all animals, and at 336 and 504 hours from the animals in cohort 2. The animals in these experiments were weight matched at 2.7 kg. Aqueous, vitreous and serum samples were stored at −80°C, and submitted for drug level concentration determinations.

Aqueous humor, vitreous humor and serum samples were analyzed using an MSD assay employing goat anti-human IgG Fc for capture and Sulfo Tag labeled goat anti-human IgG antibody for chemiluminescent detection. The assay was performed in 1% final concentration rabbit serum. Standard curve fitting and data evaluation was performed using XLfit4 software. A calibration curve was plotted from MSD luminescence units vs. theoretical standard concentrations. A four-parameter logistic model was used for curve fitting. The regression equation for the calibration curve was then used to back calculate the measured concentrations. Plates passed when at least 2/3 of the QCs were within 30% of the expected values. The linear range of the MSD assay of ABBV642 was 30–0.041 μg/mL for the serum and humor matrices. The LLOQ was 0.041 μg/mL for all assays. Values that were BQL were omitted from calculations. PK parameters were calculated with Pharmacokinetics Laboratory Automation Software for Management and Analysis (PLASMA) Version 2.6.12 (SPaRCS, AbbVie) using the linear trapezoidal method, and non-compartmental analysis.

Evaluation of preclinical efficacy of ABBV642 in subretinal neovascularization models

The animal procedures were approved by the IACUC conducted in accordance with the ARVO Statement for the Use of Animals in Ophthalmic and Vision Research. Two animal models of subretinal neovascularization, Rho/huVEGF transgenic mouse model and tet/opsin/huVEGF double transgenic mice, were used to evaluate in vivo efficacy of ABBV642.

Transgenic mice with increased expression of VEGF in photoreceptors

Transgenic mice in which the rhodopsin promoter drives expression of VEGF in photoreceptors (Rho-VEGF mice) have onset of VEGF expression at P7 and starting at P10, develop sprouts of NV from the deep capillary bed of the retina that grow through the photoreceptor layer and form an extensive network of new vessels in the subretinal space. The concentration of aflibercept (Regeneron Pharmaceuticals, Tarrytown, New York) injected into human eyes is 2 mg/ml. Intraocular injection of 1 μl of the 2 mg/ml clinical concentration, which is 0.32 μmoles of aflibercept was done and 0.32 μmoles of all other agents was injected for comparison. At P14 hemizygous Rho-VEGF mice were given an intraocular injection of 1 μl of test agent in one eye. At P21, the mice were euthanized, and eyes were fixed in 10% formalin for 2 hours. Retinas were dissected, blocked with 5% normal swine serum in PBS for 1 hour, stained with FITC-conjugated GSA (Vector Labs, Burlingame, CA) for 2 hours to stain vascular cells, flat mounted with the photoreceptor side up, and examined by fluorescence microscopy. The area of subretinal NV was measured with image analysis by an investigator blinded with respect to treatment groups.

Tet-opsin-VEGF double-transgenic mice

When given injections of doxycycline (Dox), double transgenic mice with Dox-inducible expression of VEGF express 10-fold higher levels of VEGF than Rho-VEGF transgenic mice and develop severe NV and exudative retinal detachment within 3–5 d. Adult male Tet-opsin-VEGF transgenic mice were given an intraocular injection of 0.34 μmoles of test agent in one eye and started on 50 mg/kg of Dox by subcutaneous injection once every day for 3 d. At the 4th day, wide field fundus photos were taken by Micron III retinal imaging microscope (Phoenix Research Laboratories, Pleasanton, CA). Optical coherence tomography(OCT, bioptigen) was also taken. For retina exudation/detachment that could not be decided by fundus image and OCT, cryosection was done. Images were graded by two independent observers masked with respect to treatment groups using the following grading scale: 0 = no retinal detachment (NRD), 1 = partial retinal detachment (PRD), 2 = total retinal detachment (TRD) (Fig. 7).

Disclosure of potential conflicts of interest

ORCID

Susan Marchie http://orcid.org/0000-0001-6338-4556

References

1. The Angiogenesis Foundation. Advocating for improved treatment and outcomes for wet age-related macular degeneration. 2012; https://www.angio.org/wp-content/uploads/2013/10/AMD_Final_Report_2012.pdf

2. Vinores SA, Xiao WH, Aslam S, Shen J, Oshima Y, Nambu H, Liu H, Carmeliet P, Campochiaro PA. Implication of the hypoxia response element of the Vegf promoter in mouse models of retinal and choroidal neovascularization, but not retinal vascular development. J Cell Physiol 2006; 206:749-58; PMID:16245301; http://dx.doi.org/10.1002/jcp.20525

3. Kwak N, Okamoto N, Wood JM, Campochiaro PA. VEGF is major stimulator in model of choroidal neovascularization. Invest Ophthalmol Vis Sci 2000; 41:3158-64; PMID:10967078

4. Okamoto N, Tobe T, Hackett SF, Ozaki H, Vinores MA, LaRochelle W, Zack DJ, Campochiaro PA. Transgenic mice with increased expression of vascular endothelial growth factor in the retina: a new model of intraretinal and subretinal neovascularization. Am J Pathol 1997; 151:281-91; PMID:9212753

5. Kelly BD, Hackett SF, Hirota K, Oshima Y, Cai Z, Berg-Dixon S, Rowan A, Yan Z, Campochiaro PA, Semenza GL. Cell type-specific regulation of angiogenic growth factor gene expression and induction of angiogenesis in nonischemic tissue by a constitutively active form of hypoxia-inducible factor 1. Circ Res 2003; 93:1074-81; PMID:14576200; http://dx.doi.org/10.1161/01.RES.0000102937.50486.1B

6. Rosenfeld PJ, Brown DM, Heier JS, Boyer DS, Kaiser PK, Chung CY, Kim RY, Group MS. Ranibizumab for neovascular age-related macular degeneration. N Engl J Med 2006; 355:1419-31; PMID:17021318; http://dx.doi.org/10.1056/NEJMoa054481

7. Brown DM, Campochiaro PA, Singh RP, Li Z, Gray S, Saroj N, Rundle AC, Rubio RG, Murahashi WY, Investigators C. Ranibizumab for macular edema following central retinal vein occlusion: six-month primary end point results of a phase III study. Ophthalmology 2010; 117:1124-33 e1; PMID:20381871; http://dx.doi.org/10.1016/j.ophtha.2010.02.022

8. Heier JS, Brown DM, Chong V, Korobelnik JF, Kaiser PK, Nguyen QD, Kirchhof B, Ho A, Ogura Y, Yancopoulos GD, et al. Intravitreal aflibercept (VEGF trap-eye) in wet age-related macular degeneration. Ophthalmology 2012; 119:2537-48; PMID:23084240; http://dx.doi.org/10.1016/j.ophtha.2012.09.006

9. Group CR, Martin DF, Maguire MG, Ying GS, Grunwald JE, Fine SL, Jaffe GJ. Ranibizumab and bevacizumab for neovascular age-related macular degeneration. N Engl J Med 2011; 364:1897-908; PMID:21526923; http://dx.doi.org/10.1056/NEJMoa1102673

10. Comparison of Age-related Macular Degeneration Treatments Trials (CATT) Research Group, Maguire MG, Martin DF, Ying GS, Jaffe GJ, Daniel E, Grunwald JE, Toth CA, Ferris FL. Five-Year Outcomes with Anti-Vascular Endothelial Growth Factor Treatment of Neovascular Age-Related Macular Degeneration: The Comparison of Age-Related Macular Degeneration Treatments Trials. Ophthalmology 2016 Aug; 123(8):1751-61; PMID: 27156698; http://dx.doi.org/10.1016/j.ophtha.2016.03.045

11. Grunwald JE, Daniel E, Huang J, Ying GS, Maguire MG, Toth CA, Jaffe GJ, Fine SL, Blodi B, Klein ML, et al. Risk of geographic atrophy in the comparison of age-related macular degeneration treatments trials. Ophthalmology 2014; 121:150-61; PMID:24084496; http://dx.doi.org/10.1016/j.ophtha.2013.08.015

12. Campochiaro PA, Glaser BM. Platelet-derived growth factor is chemotactic for human retinal pigment epithelial cells. Arch Ophthalmol 1985; 103:576-9; PMID:3985844; http://dx.doi.org/10.1001/archopht.1985.01050040118034

13. Seo MS, Okamoto N, Vinores MA, Vinores SA, Hackett SF, Yamada H, Yamada E, Derevjanik NL, LaRochelle W, Zack DJ, et al. Photoreceptor-specific expression of platelet-derived growth factor-B results in traction retinal detachment. Am J Pathol 2000; 157:995-1005; PMID:10980138; http://dx.doi.org/10.1016/S0002-9440(10)64612-3

14. Mori K, Gehlbach P, Ando A, Dyer G, Lipinsky E, Chaudhry AG, Hackett SF, Campochiaro PA. Retina-specific expression of PDGF-B versus PDGF-A: vascular versus nonvascular proliferative retinopathy. Invest Ophthalmol Vis Sci 2002; 43:2001-6; PMID:12037011

15. Campochiaro PA, Hackett SF, Vinores SA, Freund J, Csaky C, LaRochelle W, Henderer J, Johnson M, Rodriguez IR, Friedman Z, et al. Platelet-derived growth factor is an autocrine growth stimulator in retinal pigmented epithelial cells. J Cell Sci 1994; 107(Pt 9):2459-69; PMID:7844163

16. Lei H, Rheaume MA, Kazlauskas A. Recent developments in our understanding of how platelet-derived growth factor (PDGF) and its receptors contribute to proliferative vitreoretinopathy. Exp Eye Res 2010; 90:376-81; PMID:19931527; http://dx.doi.org/10.1016/j.exer.2009.11.003

17. Jo N, Mailhos C, Ju M, Cheung E, Bradley J, Nishijima K, Robinson GS, Adamis AP, Shima DT. Inhibition of platelet-derived growth factor B signaling enhances the efficacy of anti-vascular endothelial growth factor therapy in multiple models of ocular neovascularization. Am J Pathol 2006; 168:2036-53; PMID:16723717; http://dx.doi.org/10.2353/ajpath.2006.050588

18. Dong A, Seidel C, Snell D, Ekawardhani S, Ahlskog JK, Baumann M, Shen J, Iwase T, Tian J, Stevens R, et al. Antagonism of PDGF-BB suppresses subretinal neovascularization and enhances the effects of blocking VEGF-A. Angiogenesis 2014; 17:553-62; PMID:24154861

19. Jaffe GJ, Eliott D, Wells JA, Prenner JL, Papp A, Patel S. A phase 1 study of intravitreous E10030 in combination with ranibizumab in neovascular age-related macular degeneration. Ophthalmology 2016; 123:78-85; PMID:26499921; http://dx.doi.org/10.1016/j.ophtha.2015.09.004

20. Chakravarthy U, Jaffe GJ. Dual antagonism of platelet derived growth factor (Fovista® 1.5 mg) and vascular endothelial growth factor (Lucentis® 0.5 mg) results in reduced sub-retinal fibrosis and neovascular growth. Am Acad Ophthalmol Ann Meeting 2014, Oct. 18-21, Chicago.

21. Park SJ, Choi Y, Na YM, Hong HK, Park JY, Park KH, Chung JY, Woo SJ. Intraocular pharmacokinetics of intravitreal aflibercept (Eylea) in a rabbit model. Invest Ophthalmol Vis Sci 2016; 57:2612-7; PMID:27258433; http://dx.doi.org/10.1167/iovs.16-19204

22. Hutton-Smith LA, Gaffney EA, Byrne HM, Maini PK, Schwab D, Mazer NA. A mechanistic model of the intravitreal pharmacokinetics of large molecules and the pharmacodynamic suppression of ocular vascular endothelial growth factor levels by ranibizumab in patients with neovascular age-related macular degeneration. Mol Pharm 2016;

13:2941-50; PMID:26726925; http://dx.doi.org/10.1021/acs. molpharmaceut.5b00849

23. Gadkar K, Pastuskovas CV, Le Couter JE, Elliott JM, Zhang J, Lee CV, Sanowar S, Fuh G, Kim HS, Lombana TN, et al. Design and pharmacokinetic characterization of novel antibody formats for ocular therapeutics. Invest Ophthalmol Vis Sci 2015; 56:5390-400; PMID:26275136; http://dx.doi.org/10.1167/iovs.15-17108

24. Falavarjani KG, Nguyen QD. Adverse events and complications associated with intravitreal injection of anti-VEGF agents: a review of literature. Eye (Lond) 2013; 27:787-94; PMID:23722722; http://dx.doi.org/10.1038/eye.2013.107

25. Ghetie V, Hubbard JG, Kim JK, Tsen MF, Lee Y, Ward ES. Abnormally short serum half-lives of IgG in beta 2-microglobulin-deficient mice. Eur J Immunol 1996; 26:690-6; PMID:8605939; http://dx.doi.org/10.1002/eji.1830260327

26. Kim JK, Firan M, Radu CG, Kim CH, Ghetie V, Ward ES. Mapping the site on human IgG for binding of the MHC class I-related receptor, FcRn. Eur J Immunol 1999; 29:2819-25; PMID:10508256; http://dx.doi.org/10.1002/(SICI)1521-4141(199909)29:09%3c2819::AID-IMMU2819%3e3.0.CO;2-6

27. Lindblom P, Gerhardt H, Liebner S, Abramsson A, Enge M, Hellstrom M, Backstrom G, Fredriksson S, Landegren U, Nystrom HC, et al. Endothelial PDGF-B retention is required for proper investment of pericytes in the microvessel wall. Genes Dev 2003; 17:1835-40; PMID:12897053; http://dx.doi.org/10.1101/gad.266803

28. Ferrara N. Binding to the extracellular matrix and proteolytic processing: two key mechanisms regulating vascular endothelial growth factor action. Mol Biol Cell 2010; 21:687-90; PMID:20185770; http://dx.doi.org/10.1091/mbc.E09-07-0590

29. Hezareh M, Hessell AJ, Jensen RC, van de Winkel JG, Parren PW. Effector function activities of a panel of mutants of a broadly neutralizing antibody against human immunodeficiency virus type 1. J Virol 2001; 75:12161-8; PMID:11711607; http://dx.doi.org/10.1128/JVI.75.24.12161-12168.2001

30. Xu D, Alegre ML, Varga SS, Rothermel AL, Collins AM, Pulito VL, Hanna LS, Dolan KP, Parren PW, Bluestone JA, et al. In vitro characterization of five humanized OKT3 effector function variant antibodies. Cell Immunol 2000; 200:16-26; PMID:10716879; http://dx.doi.org/10.1006/cimm.2000.1617

31. Wu C, Ying H, Grinnell C, Bryant S, Miller R, Clabbers A, Bose S, McCarthy D, Zhu RR, Santora L, et al. Simultaneous targeting of multiple disease mediators by a dual-variable-domain immunoglobulin. Nat Biotechnol 2007; 25:1290-7; PMID:17934452; http://dx.doi.org/10.1038/nbt1345

32. Mineur P, Colige AC, Deroanne CF, Dubail J, Kesteloot F, Habraken Y, Noel A, Voo S, Waltenberger J, Lapiere CM, et al. Newly identified biologically active and proteolysis-resistant VEGF-A isoform VEGF111 is induced by genotoxic agents. J Cell Biol 2007; 179:1261-73; PMID:18086921; http://dx.doi.org/10.1083/jcb.200703052

33. Vinores SA. Pegaptanib in the treatment of wet, age-related macular degeneration. Int J Nanomedicine 2006; 1:263-8; PMID:17717967

34. Leveen P, Pekny M, Gebre-Medhin S, Swolin B, Larsson E, Betsholtz C. Mice deficient for PDGF B show renal, cardiovascular, and hematological abnormalities. Genes Dev 1994; 8:1875-87; PMID:7958863; http://dx.doi.org/10.1101/gad.8.16.1875

35. Chu H, Wang Y. Therapeutic angiogenesis: controlled delivery of angiogenic factors. Ther Deliv 2012; 3:693-714; PMID:22838066; http://dx.doi.org/10.4155/tde.12.50

36. Abramsson A, Kurup S, Busse M, Yamada S, Lindblom P, Schallmeiner E, Stenzel D, Sauvaget D, Ledin J, Ringvall M, et al. Defective N-sulfation of heparan sulfate proteoglycans limits PDGF-BB binding and pericyte recruitment in vascular development. Genes Dev 2007; 21:316-31; PMID:17289920; http://dx.doi.org/10.1101/gad.398207

37. Schindelin J, Rueden CT, Hiner MC, Eliceiri KW. The ImageJ ecosystem: An open platform for biomedical image analysis. Mol Reprod Dev 2015; 82:518-29; PMID:26153368; http://dx.doi.org/10.1002/mrd.22489

38. Ohno-Matsui K, Hirose A, Yamamoto S, Saikia J, Okamoto N, Gehlbach P, Duh EJ, Hackett S, Chang M, Bok D, et al. Inducible expression of vascular endothelial growth factor in adult mice causes severe proliferative retinopathy and retinal detachment. Am J Pathol 2002; 160:711-9; PMID:11839592; http://dx.doi.org/10.1016/S0002-9440(10)64891-2

39. Bakri SJ, Snyder MR, Reid JM, Pulido JS, Singh RJ. Pharmacokinetics of intravitreal bevacizumab (Avastin). Ophthalmology 2007; 114:855-9; PMID:17467524; http://dx.doi.org/10.1016/j.ophtha.2007.01.017

40. M.W. S. Pharmacokinetics. pharmacodynamics and pre-clinical characteristics of ophthalmic drugs that bind VEGF. Expert Rev Clin Pharmacol 2014; 7:167-80; PMID:24483136; http://dx.doi.org/10.1586/17512433.2014.884458

41. Holz FG, Tadayoni R, Beatty S, Berger A, Cereda MG, Cortez R, Hoyng CB, Hykin P, Staurenghi G, Heldner S, et al. Multi-country real-life experience of anti-vascular endothelial growth factor therapy for wet age-related macular degeneration. Br J Ophthalmol 2015; 99:220-6; PMID:25193672; http://dx.doi.org/10.1136/bjophthalmol-2014-305327